Almotiry et al | Article 9417
J Pure Appl Microbiol. 2024;18(3):1824-1837. doi: 10.22207/JPAM.18.3.30
Received: 30 March 2024 | Accepted: 27 June 2024
Published Online: 19 August 2024

P-ISSN: 0973-7510; E-ISSN: 2581-690X

RESEARCH ARTICLE OPEN ACCESS

Synthesis of UiO-67 Metal-organic Frameworks (MOFs) and their Application as Antibacterial and Anticancer Materials

Sitah Almotiry[1,2], Mehal AlQriqri[3], Basma Alhogbi[1], Salah E.M. Abo-Aba[4,5], Mariusz Jaremko[6] and Mohamed Abdel Salam[1]*

[1]Chemistry Department, Faculty of Science, King Abdulaziz University, P.O Box 80200- Jeddah 21589, Saudi Arabia.
[2]Department of Chemistry, College of Science, Qassim University, Buraidah 51452, Saudi Arabia.
[3]Regenerative Medicine, King Fahad Medical Research Center, King Abdulaziz University, Jeddah, Saudi Arabia.
[4]Biological Science Department, Faculty of Science, King Abdulaziz University, P.O Box 80200- Jeddah 21589, Saudi Arabia.
[5]Princess Dr. Najlal Bent Saud Al Saud Centre for Excellence Research in Biotechnology, Jeddah, Saudi Arabia.
[6]Biological and Environmental Science and Engineering (BESE) Division, King Abdullah University of Science and Technology (KAUST), P.O. Box 4700, Thuwal, Makkah, Saudi Arabia.

Abstract

This study involved the synthesis of the UiO-67 metal-organic framework; UiO-67 is a well-known type of MOF obtained by coordinating the $Zr_6O_4(OH)4$ metal unit with the 4,42-biphenyldicarboxylate organic linker, using the hydrothermal technique. The novelty of the current work is to synthesize UiO-67 MOFs, and their application as biological agents for antibacterial and cancer cells. Subsequently, the composite material UiO-67 was subjected to a comprehensive characterization process involving Fourier-transform infrared spectroscopy (FTIR), scanning electron microscopy (SEM), thermal gravimetric analyses (TGA) and surface area analysis, and the results showed the successful synthesis of the UiO-67 MOFs, with a high specific surface area of 1415 m^2/g. The synthesized UiO-67 for its antibacterial properties tested against five pathogenic bacterial strains, which include three gram-positive and mcillin-resistant pairs including MRSA, *S. aureus* and *Enterococcus faecalis,* and Two gram-negative bacteria *E. colli* and *S. typhimurium* using the agar well diffusion method. These findings have shown enhanced, strong antibacterial activity against all the five used gram-positive and gram-negative bacterial strains. Furthermore, the anticancer efficacy of UiO-67 was evaluated on two distinct types of cancer cells: We are using MCF-7 (human breast cancer cell line) and HepG2 (human liver cancer cells). The experiments prove that UiO-67 has the potential of cytotoxicity against both Glioblastoma and H460 cancer lines with the ability to inhibit apoptosis at the same time.

Keywords: UiO-67, Hydrothermal Technique, Antibacterial, Anticancer

***Correspondence:** masalam16@hotmail.com

Citation: Almotiry S, AlQriqri M, Alhogbi B, Abo-Aba SEM, Jaremko M, Salam MA. Synthesis of UiO-67 Metal-organic Frameworks (MOFs) and their Application as Antibacterial and Anticancer Materials. *J Pure Appl Microbiol.* 2024;18(3):1824-1837. doi: 10.22207/JPAM.18.3.30

INTRODUCTION

MOFs, are considered as the future generation of anti-bacterial agents, which are known as metal-organic frameworks. They have the advantages of a large specific surface area, adjustability of pore structure, and a controlled rate of ion release compared to other standard bactericidal materials.[1,2] Thus, Metal-organic frameworks (MOFs) have vast prospects in the future as they can be used in applications like food, storage, health detection, antifungal and bacterial layering, and water purification. MOFs, fused for (Metal-Organic Frameworks,), are a group of porous materials that are created through the process of self-assembly of ligands that incorporate organic species and metal ions.[3] These are materials formed from metal ions and molecules used to build links between them the linkers are organic.[4-6] The metal ion centers are coordinated with the organic ligands either through coordination or covalent interactions, which provide a complex network morphology. The metal ions and ligands can have any geometric configuration, from spheres to polygons and pyramids, and are connected in various forms. Hence, the physicochemical characteristics of MOFs may be intentionally engineered and modified to suit diverse applications.[7] MOFs may be synthesized with not just great porosity, but also a diverse range of pore geometries. The flexibility and surface area of the framework in MOFs can be determined by manipulating the composition, size, structure, and shape of the organic ligands. This can lead to the formation of a final permeable substance that is highly suitable for a range of special requirements.[8-11] During the first phases of MOFs development, its primary uses were focused on catalysis, separation, and gas mixture storage.[12,13]

Nevertheless, the utilization of MOF is now broadening to encompass energy storage devices, sensor detection, adsorption of hazardous materials, novel catalysis, and biological applications.[14-18] The preparation techniques for MOFs have undergone continual evolution because of their wide-ranging potential for application. Currently, a wide range of techniques have been documented for the production of MOFs, including solvothermal hydrothermal methods, son chemical synthesis, electrochemical synthesis, microwave-assisted synthesis, mechanochemical synthesis, ionothermal synthesis processes, microfluidic synthesis, and dry gel conversion.[19-23]

The MOFs of UiO-67 are a member of the UiO Zr-MOF family, which is characterized by its microporous nature.[24-27] This type of MOF has wide applications due to its thermal and chemical composition and mechanical stability.[28-30] The stability of this group of Metal-Organic Frameworks (MOFs) is evidenced by the elevated oxidation state of Zirconium (IV) in comparison to other categories of MOFs.[31] The UiO-type MOFs exhibit remarkable chemical, thermal (able to endure temperatures equal to 500°C), and dynamic robustness.[32] The UiO-67 MOFs possess a face-centered cylindrical (fcc) configuration, formed by linking an inorganic octagonal Zr6 unit to 12, an inorganic subunit.[33] In addition, the presence of small, porous triangular openings allows for entry into super tetrahedral cages with a size of 12 Å and super octahedral cages with a size of 16 Å.[34] UiO-67 demonstrates exceptional properties, including an increased BET area on the surface and microspore volume, as well as a lower density.[35]

The novelty of the current study involved the synthesis, and characterization of the UiO-67 metal-organic frameworks and explored their antibacterial and anticancer activities. The morphological and structural characteristics of the synthesized UiO-67 were investigated. In addition, the antibacterial efficacy of UiO-67 against five pathogenic bacteria, consisting of three types of gram-positive *MRSA, Enterococcus faecalis, S. aureus* and two types of gram-negative bacteria, *E. coli and S. typhimurium*, was assessed using agar plates diffusion well test. The anticancer potential of synthesized UiO-67 was investigated on MCF-7 (human breast cancer) and HepG2 (human liver cancer) cells, as these types of cancer pose significant health issues globally.

MATERIALS AND METHODS

Materials

The chemical substances employed in the production of UiO-67 include Zirconium tetrachloride ($ZrCl_4$), 4,42-biphenyldicarboxylic acid (BPDC), acetic acid, hydrochloric acid (HCl)

at a concentration of 37%, dimethylformamide (DMF), and acetone, all of which were obtained from Sigma-Aldrich Co. The microorganisms selected to evaluate antibacterial activity were Gram-positive bacteria MRSA, *S. aureus,* and *Enterococci,* as well as Gram-negative bacteria *E. coli* and *S. typhimurium*. These bacteria were obtained from the Medicines Research Center, King Fahad, in Jeddah, Saudi Arabia. Bacterial cultures were preserved using Nutrient agar slants obtained from Himedia, India. The MCF-7 cell line (derived from human breast cancer) and the HepG2 cell line (derived from human liver cancer) samples were acquired from the Regenerative Medicine unit of King Fahad Medical Research Center. MCF-7 and HepG2 cells were grown in DMEM media (biosera_france) supplemented with a 10% volume of fetal bovine serum (FBS, which is: biosera-france) and 5% antibiotics (the antibiotic penicillin) (biosera-france). The cells were maintained in a 5% CO_2 incubator at 37°C. Cell viability was assessed using the Cell Counting MTT test kit from Dojindo, Japan.

Preparation of UiO-67

The UiO-67 metal-organic framework (MOF) was synthesized according to Katz et al.[35] using a mixture of Zirconium tetrachloride (233 mg, 1 mmol), 4,42-biphenyldicarboxylic acid (BPDC, 242 mg, 1 mmol), acetic acid (0.6 g, 10 mmol), and hydrochloric acid (37%, 12 M; 0.16 mL, 2 mmol) were mixed in 30 mL of N, N-dimethylformamide (DMF) using the method of sonication. The solution was subjected to a temperature of 120°C for 48 hours. Subsequently, the UiO-67 white product was obtained by the process of centrifugation and subjected to three rounds of washing with DMF. The UiO-67 material, in its original form, was immersed in dimethylformamide (DMF) at ambient temperature for 6 hours in order to eliminate any residual BPDC that was not bound. Subsequently, the particles that were acquired underwent several washes with acetone in order to facilitate the displacement of the entrapped DMF, followed by a drying process at a temperature of 100°C for 24 hours.

Characterization of UiO-67

The thermal gravimetric analyses (TGA) were conducted using a TG/SDTQ600 instrument under atmospheric conditions, with temperatures ranging from 0 to 900 K. The materials' morphology was analyzed using scanning electron microscopy (SEM). The FT-IR spectra were acquired using an FTIR spectrophotometer (Spectrum 100, Perkin Elmer, Shelton, CT, USA). The zeta potential was assessed by quantifying the electrophoretic mobility of the particles with a Zeta sizer (Malvern, Massachusetts Instruments GmbH, Malvern WR14 1XZ UK).

Antibacterial activity

The bacterial strains *S. Typhimurium, E. coli, Enterococcus faecalis, Staphylococcus aureus,* and MRSA have been isolated and identified by the biological Science department at King Abdulaziz University under accession no. 14028, 11775, 29212, 12600, and 33591, respectively. The antibacterial effect was evaluated using the agar well dissemination method. In the agar well diffusion assay, the bacteria were propagated by uniformly distributing a tiny quantity of each bacterial strain on a nutrient agar plate and allowing it to grow for a whole night at a temperature of 37°C. The bacterial cultures were then separately mixed with clean sodium chloride solution (B. Braun, Germany) until they reached a turbidity level that matched the 0.5 McFarland standard. Subsequently, bacterial cultures were evenly distributed over Mueller-Hinton agar and circular holes with a diameter of approximately 7 millimeters were made on every plate of agar using a cork-borer. Each well was filled with 0.1 mL of UiO-67 at five different concentrations. The wells were then incubated for 24 h at 37°C. The measurement of bacterial growth inhibition was quantified in mm. The antimicrobial activity assays were performed three times, and the diameters millimeters of the inhibition zones were evaluated to assess the vulnerability of the bacteria to the UiO-67 MOFs.

Cytotoxicity Studies of UiO-67

MCF-7 and HepG2 cells were cultured in DMEM media with 10% fetal bovine serum (FBS) and 5% antibiotics penicillin. The cells were incubated at 37°C in an atmosphere of 5% CO_2.

MCF-7 and HepG2 cells were placed in 96-well plates with a density of 4,000 and 5,000 cells for each well, respectively. The cells were

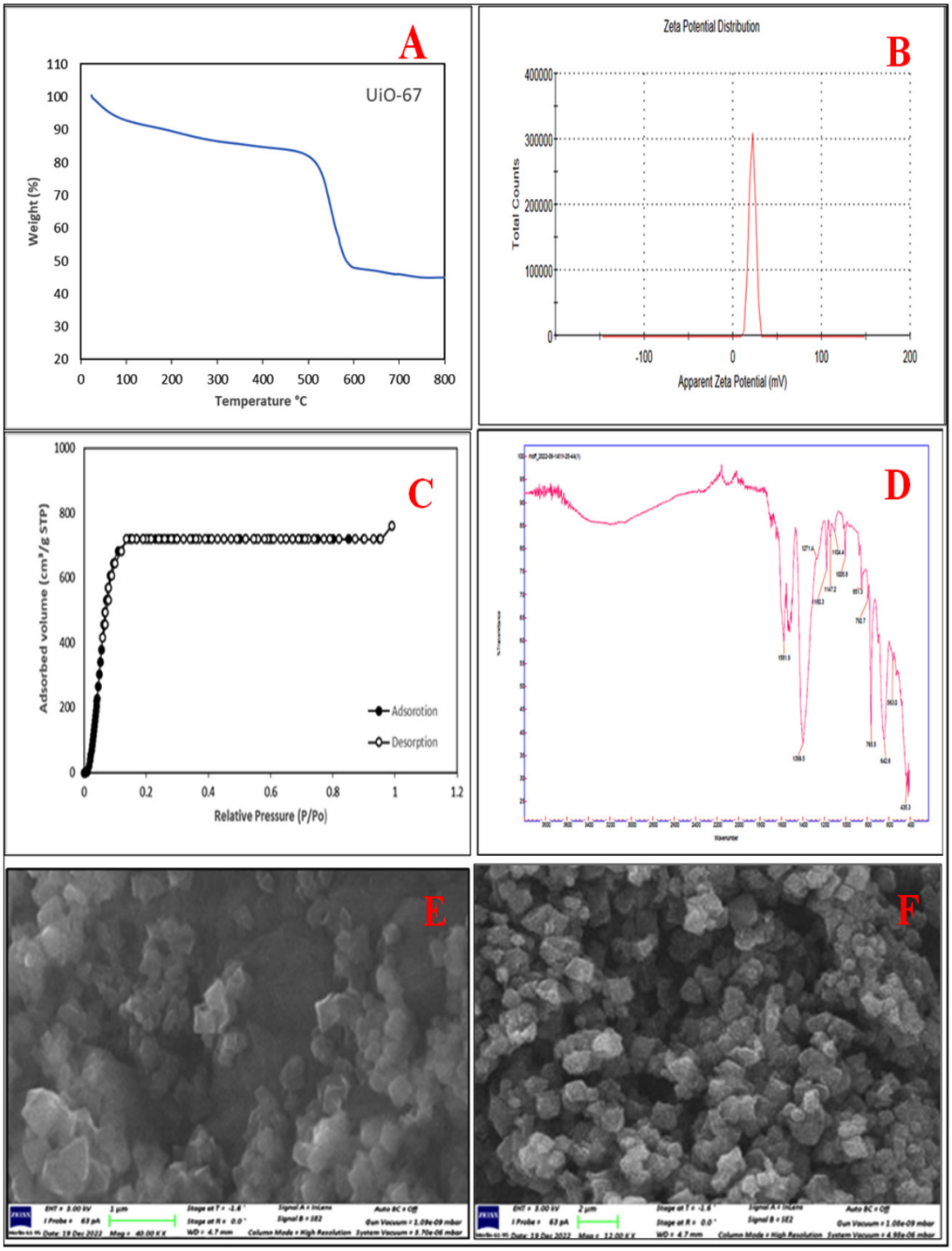

Figure 1. (A) Thermogravimetric Analysis (TGA) of UiO-67, (B) the zeta potential measurement of UiO-67, (C) N2 adsorption/desorption isotherms of UiO-67 at 77K, (D) FT-IR spectrum of UiO-67, (E) and (F) SEM images of UiO-67.

cultivated in 200 µl of DMEM enriched in 10% FBS and 5% antibiotic penicillin. After a 24-hour interval, the cells were subjected to various concentrations of UiO-67 (2, 8, 10, 30, 50, 70, 100, and 150 µg/mL) that were diluted with the growth medium. Duplicates were created for each concentration. The cells were subsequently incubated at a temperature of 37°C for durations of 24, 48, and 72 hours.

Following this, 10 µl of the MTT assay was introduced and incubated for 3 h at the same temperature. Subsequently, the optical density of the sample was measured using a microplate reader (BioTek-ELx808) at a wavelength of 450 nm. The average values of three measurements were computed, and growth curves were subsequently shown.

RESULTS AND DISCUSSION

UiO-67 MOFs characterization

A thermal gravimetric analysis (TGA) was has been carried out on a sample of UiO-67. As depicted in Figure 1A, the thermal gravimetric analysis (TGA) of the specimen exhibits three distinct phases: initial evaporation of the solvent at around 100°C, subsequent removal of the compensatory agent at around 450°C, and eventual disintegration of the framework within the temperature range of 450 to 600°C. In light of the structural characteristics of hypothesis UiO-67, this study examines the percentage of mass loss (% ZrO_2) during the temperature range of 450 to 600°C, which was around 65%. The UiO-67 material had an average Zeta Potential value of +20.8 mV, indicating a satisfactory level of stability (Figure 1

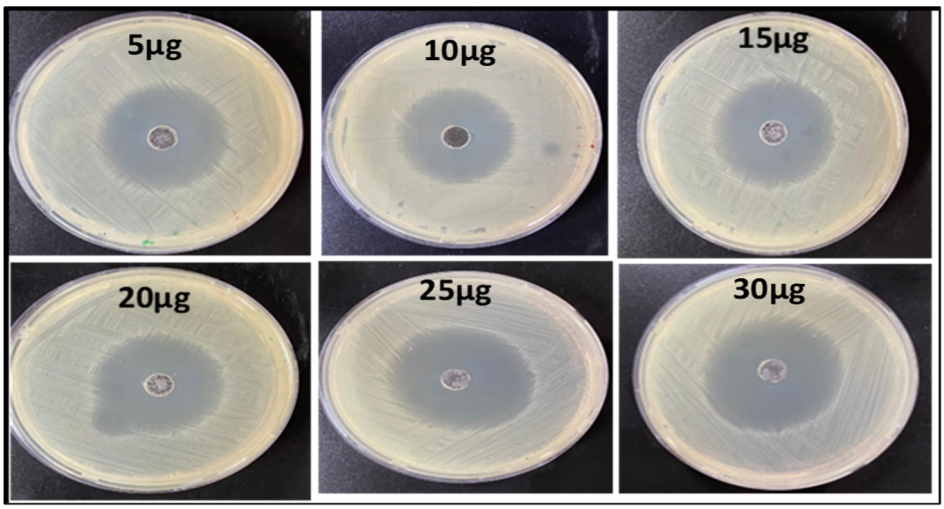

Figure 2. The inhibition zones at different concentrations of UiO-67 against the *S. typhimurum*

Table. The diameter of the area of inhibition produced by UiO-67 versus the tested bacterial pathogens

Microorganisms	Zone of inhibition (mm)					
	UiO-67 concentration					
	5 µg/mL	10 µg/mL	15 µg/mL	20 µg/mL	25 µg/mL	30 µg/mL
S. typhmurium	38 ± 0.1	39 ± 0.2	40 ± 0.4	41 ± 0.2	44 ± 0.1	45 ± 0.1
E. coli	33 ± 0.4	36 ± 0.1	39 ± 0.1	40 ± 0.3	41 ± 0.2	43 ± 0.3
Enterococcus faecalis	32 ± 0.1	32 ± 0.4	35 ± 0.2	38 ± 0.2	39 ± 0.5	40 ± 0.1
Staphcoccus aureus	39 ± 0.3	41 ± 0.3	42 ± 0.3	43 ± 0.1	45 ± 0.2	47 ± 0.2
MRSA	33 ± 0.2	33 ± 0.2	37 ± 0.1	39 ± 0.2	42 ± 0.2	45 ± 0.2

B). A higher magnitude of Zeta Potential signifies enhanced physical colloidal stability as a result of electrostatic repulsion among the constituent particles. The N_2 adsorption-desorption isotherms are shown in Figure 1C, UiO-67 demonstrates a type-I isotherm, indicating that it is a characteristic microporous material, with BET-specific surface area of 1415 m^2/g. The FTIR spectra are presented in Figure 1D, the absorption bands at 3382 cm^{-1} were ascribed to hydrogen bonding. The peaks detected at 1600 and 1581 cm^{-1} were assigned to the coordinated carboxylate groups (COO-). The strong peak detected at 1418 cm^{-1} was assigned to the skeletal vibrations of the benzene ring (C=C). SEM depicts the morphology of UiO-67 in Figure 1E and F, where the octahedral structure of Zr-MOF crystals is visible with an average crystal dimension of 450 nm.

Antibacterial activity of UiO-67

The antibacterial activities of synthesized UiO-67 were evaluated and compared against five particular pathogenic bacterial strains using the Agar well diffusion assay method. The three types of gram-positive bacteria that were detected are Mcillin-resistant *Staphylococcus aureus* (MRSA), *Staphylococcus aureus* (*S. aureus*), and *Enterococcus faecalis.* The two gram-negative

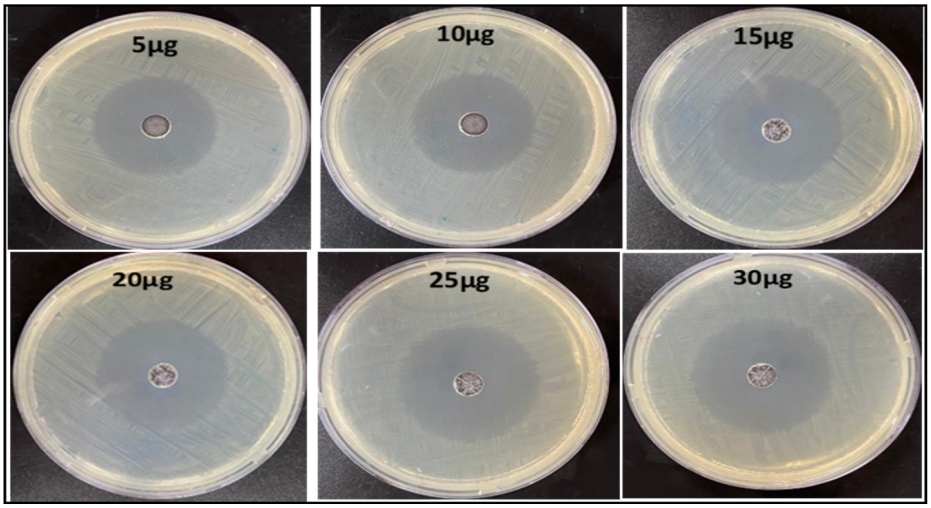

Figure 3. The inhibition zones at different concentrations of UiO-67 against the *E. coli*

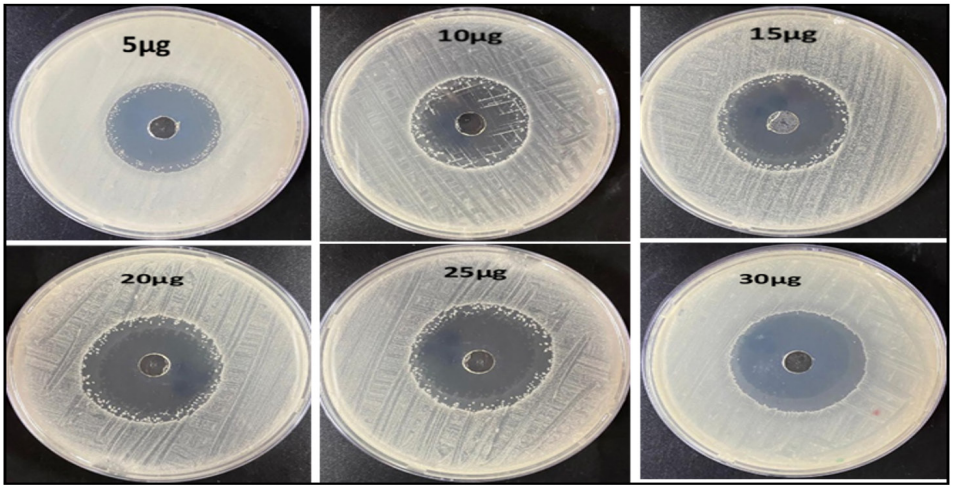

Figure 4. The inhibition zones at different concentrations of UiO-67 against the *Enterococcus faecalis*

bacteria identified were *Escherichia coli* (*E. coli*) and *Salmonella enterica Serovar typhimurium* (*S. typhimurium*). While the precise mechanism by which UiO-67 acts against bacteria remains uncertain, the prevailing theories suggest that the nanoparticles interact with bacterial membrane

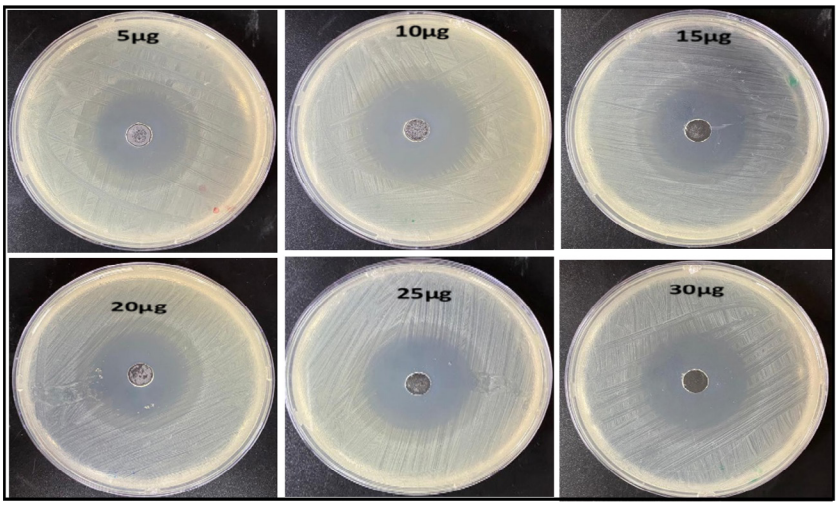

Figure 5. The inhibition zones at different concentrations of UiO-67 against the *S. aureus*

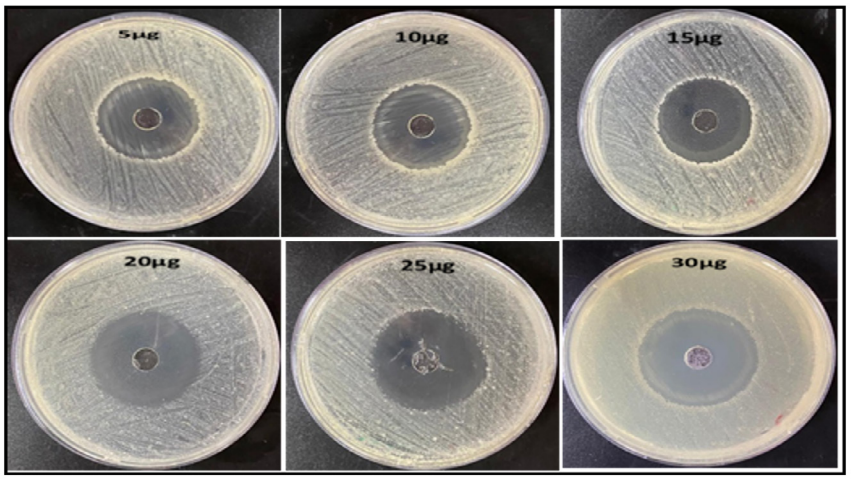

Figure 6. The inhibition zones at different concentrations of UiO-67 against the *MRSA*

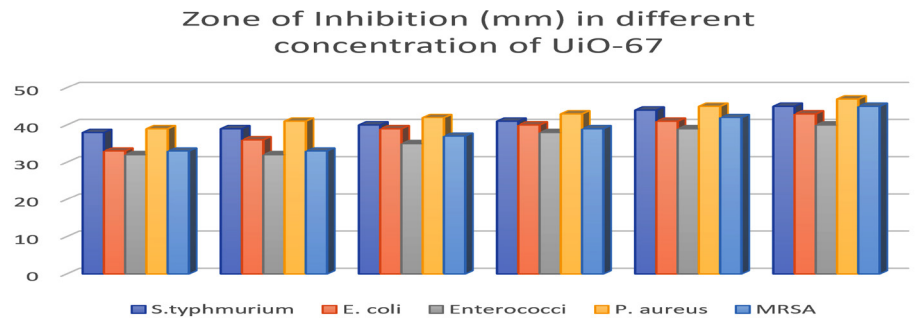

Figure 7. The inhibition zones at different concentrations of UiO-67 against different bacteria strains

proteins, leading to cell death. This occurs by penetrating the cell membrane and targeting the enzymes responsible for cell division. The UiO-67 samples that were created exhibit a greater ratio of surface area to volume, as verified by scanning electron microscopy (SEM) and surface area analysis. Hence, the contact between UiO-67 and bacterial surfaces is unavoidable, potentially leading to an increase in the antibacterial effectiveness of UiO-67.

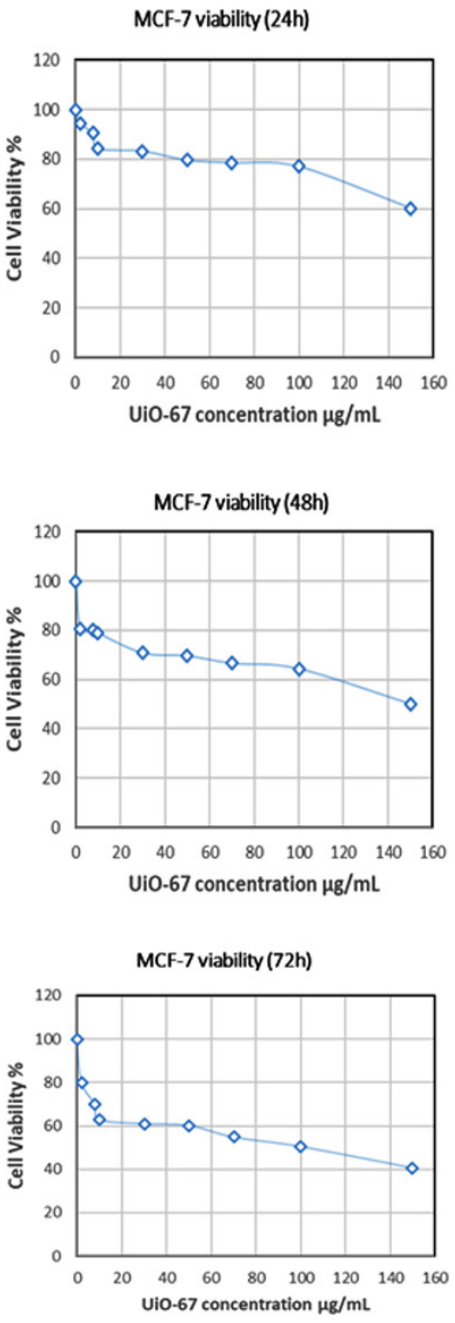

Figure 8. The percentage of cancer cell viability on the MCF-7 cell line at different concentrations and time intervals of UiO-67 MOFs

In order to validate the theory stated above, the susceptibility of the bacteria was assessed using various concentrations of UiO-67 (5, 10, 15, 20, 25, 30 µg/mL, respectively). The agar well diffusion susceptibility findings, as observed, are presented in Figure 2 to Figure 6, displaying zones of inhibition. The measurements were taken to determine the measurements of the diameter of the areas of inhibition surrounding the wells, which varied depending on the sensitivity of UiO-67. The antibacterial efficacy of UiO-67 was evaluated by quantifying the area of bacterial growth inhibition at concentrations of 5, 10, 15, 20, 25, and 30 µg/mL, respectively, reached 38 ± 1 mm, 39 ± 2 mm, 40 ± 4 mm, 41 ± 2 mm, 44 ± 1 mm and 45 ± 1 mm for *S. typhimurium*, 33 ± 4 mm, 36 ± 1 mm, 39 ± 1 mm, 40 ± 3 mm, 41 ± 2 mm and 43 ± 3 mm for *E. coli*, 32 ± 1 mm, 32 ± 4 mm, 35 ± 2 mm, 38 ± 2 mm, 39 ± 5 mm and 40 ± 1 mm for *Enterococci*. Also, The antibacterial activity, based on the zone of inhibition, has reached 39 ± 3 mm, 41 ± 3 mm, 42 ± 3 mm, 43 ± 1 mm, 45 ± 2 mm, and 47 ± 2 for *S. aureus* and 33 ± 2 mm, 33 ± 2 mm, 37 ± 1 mm, 39 ± 2 mm, 42 ± 2 mm and 45 ± 2 mm for *MRSA*. The sensitivity of the selected bacteria to UiO-67 can be ranked in the following order: *S. aureus* > *S. typhimurium* = MRSA > *E. coli* > *Enterococcus faecalis*, as shown in Table and Figure 7.

The aforementioned results demonstrated the exceptional and effective suppression of the bacterial growth activity of the UiO-67 MOFs for all studied strains (gram-positive and gram-negative bacteria), indicating the wide-spectrum effect of the UiO-67 MOFs and its ability to penetrate the cell wall of the gram-negative bacterium. The gram-positive bacterium is characterized by a thick cell wall composed of multiple layers of peptidoglycan; this cell wall is penetrated by MOFs, which are able to interact with the bacterium and facilitate its destruction. The inhibitory mechanism for the UiO-67 MOFs could have been linked to many reasons. Firstly, this could be attributed to

the generation of ROS (reactive oxygen species) such as O_2^{-2} (peroxide), H_2O_2 (hydrogen peroxide), and OH^- (hydroxyl radicals). The ROS has the potential to harm and destroy the bacterial cell due to the specific interaction between the UiO-67 MOFs and the cell organelles. Also, the bacterial membrane contains phospholipids that can be attacked and radically oxidation by ROS, destroying the membrane. Additionally, ROS can also affect any polymer part by being able to damage DNA/RNA and proteins.[36] Possibly, the interaction of the Zr ions with the phosphate group in the lipid layers. led to the destruction of the bacterium cell membrane. This interaction destroys the cell membrane and causes a leakage. Moreover, MOFs, in general, exhibit fast reactivity even at low concentrations, comparable to bleach. This can be attributed to their strong affinity for larger surface areas. For instance, MOFs with high surface area, such as UiO-67 (which has a surface area of 1415 m^2/g), are particularly effective in this regard, supported by the fact that MOFs have the advantage of two locations for interaction with the bacteria: the outer surface, which contains the organic ligands, and inner surface, which contains the metal.[37] In addition, an alternative antibacterial mechanism has been proposed, which relies on the physical interaction between the MOFs and bacteria through electrostatic or hydrophobic interactions. This interaction leads to the disruption of the cell membrane and deactivation of the intracellular substances, resulting in effective antibacterial properties.[38]

One of the findings of this research work is the outstanding inhibition of the bacteria based on the diameter of the inhibition zone, as most of the bacteria had inhibition zones more than 40 mm, with the highest value of 47 mm for the P., which is higher than any of the reported MOFs.[36,39-41] The presence of Zr ions in the middle of the MOFs may disrupt the negatively charged bacterial cell wall. This disruption is caused by the positively charged zirconium ions, leading to cell death. The electromagnetic attractions between MOFs and bacteria result in oxidation, which ultimately causes the bacteria to die.[42] Therefore, UiO-67 MOFs have the potential to be used as a more effective substitute for traditional antibiotics in combating bacterial resistance.

Cytotoxicity and anticancer studies of UiO-67

The cytotoxicity of UiO-67 MOFs was assessed on two types of human cancer cells, specifically, MCF-7 cells derived from breast cancer and HepG2 cells derived from liver cancer.

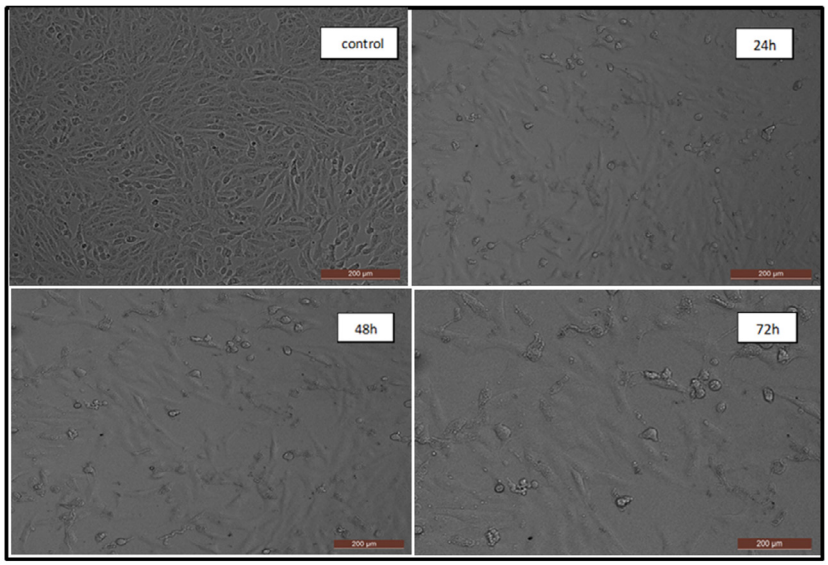

Figure 9. The changes in the structure and form of the MCF-7 cell line caused by the impact of UiO-67 MOFs at 150 µg/mL

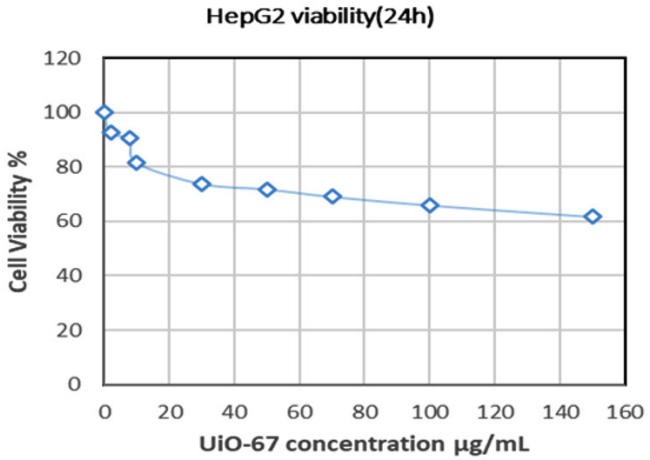

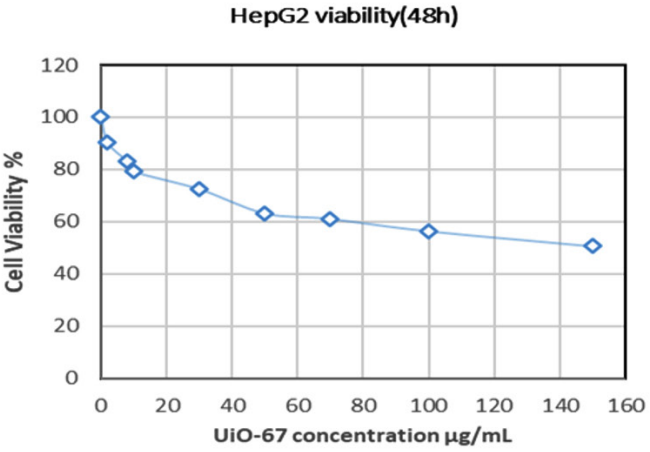

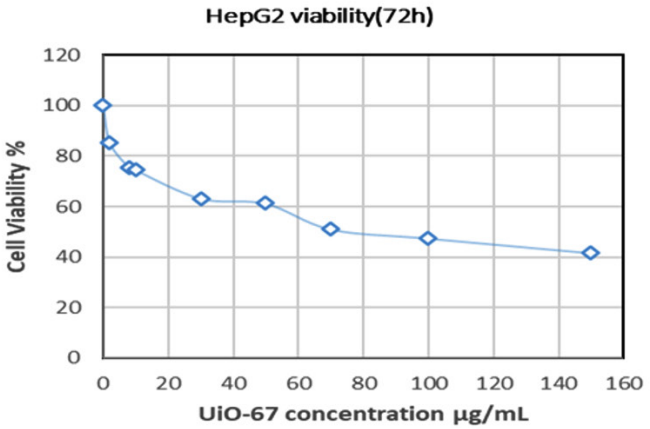

Figure 10. The percentage of cancer cell viability on the Hep G2 cell line at different concentrations and time intervals of UiO-67 MOFs

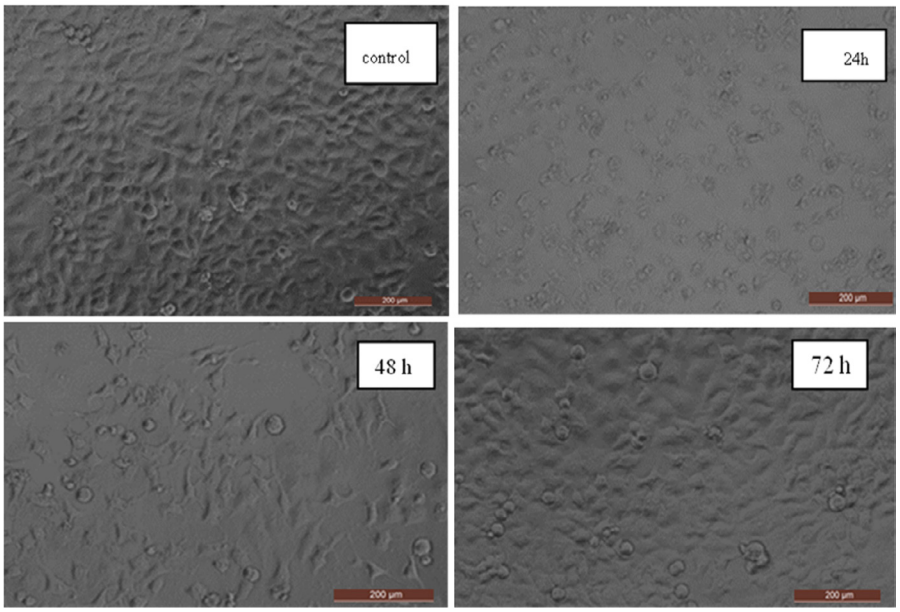

Figure 11. The changes in the structure and form of the Hep G2 cell line caused by the impact of UiO-67 MOFs at 150 µg/mL

Cell viability of human breast cancer cells (MCF-7)

The viability of human breast cancer cells was examined in the presence of UiO-67 MOFs using an MCF-7 cell line. The findings demonstrated that the synthesized UiO-67 had a remarkable cytotoxic impact on the MCF-7 cell line, as evidenced by observed morphological alterations in the MCF-7 cells, as seen in Figure 8. Furthermore, the findings demonstrated a correlation between the dosage and the observed behavior when various concentrations of UiO-67 MOFs were employed, namely 2.0, 8.0, 10, 30, 50, 70, 100, and 150 µg/mL at 24, 48, and 72 hours. Figure 9 displayed the visual depiction and structural alterations caused by the influence of UiO-67 MOFs on the MCF-7 cancer cells at 24, 48, and 72 hours. The results described a dose-dependent manner as there was a notable decrease in the survival of cells after being treated with the UiO-67 MOFs, and the maximum effect by a MOFs concentration was reached at 150 µg/mL with a % cell viability of 60%. The same manner was observed as a function of time, as the apoptosis of the cancer cell became more pronounced with the treatment time, and the cell viability reached 60.0%, 51.0%, and 40.1% by the concentration of MOFs measured at 150 µg/mL after 24, 48, and 72 hours.

Cell viability of Human liver cancer cells (HepG2)

The study investigated the cytotoxic effect of UiO-67 nanoparticles on HepG2 cells, a type of human liver cancer. Human liver cancer is of particular interest because of the global prevalence of liver cancer as a major health concern. Figure 10 shows the dose-response relationship of UiO-67 at different concentrations ranging from 2, 8, 10, 30, 50, 70, 100, and 150 µg/mL at 24, 48, and 72 hours. The findings demonstrated a notable decline in the viability of cells following the intervention, and UiO-67 MOFs showed marked cytotoxicity against the HepG2 cell line, resulting in marked changes in the cellular structure of HepG2 cells. Figure 11 depicts a visual depiction of the structural changes resulting from the effect of UiO-67 nanoparticles on cancer cells. Also, the results demonstrated a clear relationship between the dose of UiO-67 MOFs and the subsequent loss in cell viability. They reached their maximum effect by a MOFs concentration of 150 µg/mL with % a cell viability of 61%. The same manner was observed as a function of time, as the apoptosis

of the cancer cell became more pronounced with the treatment time, and the cell viability reached 61.0%, 50.0%, and 40.5% by the concentration of MOFs measured at 150 µg/mL after 24, 48, and 72 hours.

Although UiO-67 MOFs have been used for cancer treatment, they were mostly used as drug carriers,[43-45] and the cytotoxicity mechanism has not been completely investigated. The MOF nanoparticles were found to induce cancer cell death through apoptosis, specifically by activating the mitochondria-dependent pathway. This was achieved by the accumulation of the nanoparticles within the mitochondria of the cancer cells, causing the release of cytochrome C and triggering a series of apoptosis reactions involving proteins such as caspase-3 and -9,[46] which was the case with Cu-MOFs,[47] and hydroxyapatite nanoparticles.[48-49] Another explanation could be the generation of ROS due to the interaction of the MOFs with the cancer cells, which suppress the cellular immune response, leading to cell death by apoptosis.[50] It is important to highlight that when the creation of ROS exceeds the cell's ability to defend against it with antioxidants, it can trigger oxidative stress in biomolecules, ultimately resulting in cell death.[51] Additionally, studies show that NPs elicit toxic effects in macrophages by disrupting the cytoskeleton and phagocytosis, while also enhancing DNA damage linked with methylglyoxal.[52] Accordingly, the aforementioned results validate that synthesized UiO-67 metal-organic frameworks (MOFs) exhibited a preference for inducing apoptosis in cancer cells MCF-7 and Hep G2. These MOFs hold potential as a viable treatment for cancer, particularly in human breast cancer cells and liver cancer.

CONCLUSION

UiO-67 MOFs were synthesized with the hydrothermal method, and after that, the samples were characterized using FTIR, SEM, TGA, and surface area analyzer. The findings showed the synthesis of the UiO-67 MOFs thus having a high surface area of 1415 m^2/g. UiO-67 MOFs' antibacterial function has been investigated against Gram-positive bacteria like MRSA, *S. aureus*, and enterococci and the negative ones like *E. Coli* and *S. typhimurium*, among others, to determine their biological function. The outcomes reflected that the proliferation of the gram-positive and gram-negative bacterial cells was highly reduced when UiO-67 MOFs were present. Also, on the cellular metabolism suppression and ultimate bacterial death, the increase in bacterial membrane permeability was pointed out to allow abrasive UiO-67 particles, to enter the bacterial cells in a dose-dependent fashion where increasing the amounts of UiO-67 had the effect of increasing the results in this regard. Moreover, the cytotoxicity of UiO-67 on two types of human cancer cells was investigated Wherein, MCF-7 is a human breast cancer cell line, and is the human liver cancer cells. The results revealed that UiO-67 particles interact greatly with both cancer cells, suppressing cellular defense mechanisms, so triggering the apoptotic process, ultimately resulting in cell death, in a dose-dependent manner as increasing the concentration of UiO-67 further amplified these effects, as well as time-dependent manner. The findings indicate that UiO-67 MOFs exhibit great potential as a material for medicinal applications, particularly in the treatment of bacterial infections and cancer.

ACKNOWLEDGEMENTS

None.

CONFLICT OF INTEREST

The authors declare that there is no conflict of interest.

AUTHORS' CONTRIBUTION

All authors listed have made a substantial, direct and intellectual contribution to the work, and approved it for publication.

FUNDING

None.

DATA AVAILABILITY

All datasets generated or analyzed during this study are included in the manuscript.

ETHICS STATEMENT

This article does not contain any studies on human participants or animals performed by any of the authors.

REFERENCES

1. Yao T, Zeng X, Tao X, Xu H. Recent progress of MOF-based antibacterial hydrogels. *Chem Eng J.* 2024;487:1385-8947.doi: 10.1016/j.cej.2024.150641
2. Bigham A, Islami N, Khosravi A, Zarepour A, Iravani S, Zarrabi A. MOFs and MOF-Based Composites as Next-Generation Materials for Wound Healing and Dressings. *Small.* 2024:e2311903. doi: 10.1002/smll.202311903
3. Umemura A, Diring S, Furukawa S, Uehara H, Tsuruoka T, Kitagawa S. Morphology design of porous coordination polymer crystals by coordination modulation. *J Am Chem Soc.* 2011;133(39):15506-15513. doi: 10.1021/ja204233q
4. Li J-R, Sculley J, Zhou H-C. Metal–organic frameworks for separations. *Chem Rev.* 2012;112(2):869-932. doi: 10.1021/cr200190s
5. Zhao X, Wang Y, Li D, Bu X, Feng P. Metal–organic frameworks for separation. *Adv Mater*. 2018;30(37):1705189. doi: 10.1002/adma.201705189
6. Meek ST, Greathouse JA, Allendorf MD. Metal organic frameworks: A rapidly growing class of versatile nanoporous materials. *Adv Mater*. 2011;23(2):249-267. doi: 10.1002/adma.201002854
7. Chen W, Wu C. Synthesis, functionalization, and applications of metal-organic frameworks in biomedicine. *Dalton Transactions.* 2018;7:2114-2133. doi: 10.1039/c7dt04116k
8. Furukawa H, Cordova KE, O'Keeffe M, Yaghi OM. The chemistry and applications of metal-organic frameworks. *Science.* 2013;341(6149):1230444. doi: 10.1126/science.1230444
9. Mori W, Takamizawa S, Li D-S. Microporous materials of metal carboxylates. *J Solid State Chem.* 2000;152:120-129.
10. Beg S, Rahman M, Jain A, et al. Nanoporous metal organic frameworks as hybrid polymer–metal composites for drug delivery and biomedical applications. *Drug Discov Today.* 2017;22(4):625-637. doi: 10.1016/j.drudis.2016.10.001
11. Horcajada P, Gref R, Baati T, et al. Metal–organic frameworks in biomedicine. *Chem Rev.* 2012;112(2):1232-1268. doi: 10.1021/cr200256v
12. Felix SA, Prabu J, Maniraj H, et al. Metal–Organic Frameworks (MOFs): The Next Generation of Materials for Catalysis, Gas Storage, and Separation. *J Inorg Organomet Polym.* 2023;33(7):1757-1781.doi: 10.1007/s10904-023-02657-1
13. Yu S, Li C, Zhao S, Chai M, Hou J, Lin R. Recent advances in the interfacial engineering of MOF-based mixed matrix membranes for gas separation. *Nanoscale.* 2024;16:7716-7733. doi: 10.1039/D4NR00096J
14. Zhou Y, Li P, Wang Y, Zhao Q, Sun H. Progress in the Separation and Purification of Carbon Hydrocarbon Compounds Using MOFs and Molecular Sieves. *Separations*. 2023;10(10):543. doi: 10.3390/separations10100543
15. Tolkou AK, Zouboulis AI. Fluoride Removal from Water Sources by Adsorption on MOFs. *Separations.* 2023;10(9):467.doi: 10.3390/separations10090467
16. Paitandi RP, Wan Y, Aftab W, Zhong R, Zou R. Pristine Metal–Organic Frameworks and their Composites for Renewable Hydrogen Energy Applications. *Adv Funct Mater.* 2023;33(8):2203224.
17. Kari NEF, Ismail M, Ahmad A, Kamal K, Chew TL, Bustam MA. Screening and Experimental Validation for Selection of Open Metal Sites Metal-Organic Framework (M-CPO-27, M = Co, Mg, Ni and Zn) to Capture CO_2. *Separations.* 2023;10(8):434. doi: 10.3390/separations10080434
18. Sohrabi H, Ghasemzadeh S, Ghoreishi Z, et al. Metal-organic frameworks (MOF)-based sensors for detection of toxic gases: A review of current status and future prospects. *Mater Chem Phys.* 2023;299:127512.
19. Fan M, Yan J, Cui Q, et al. Synthesis and peroxide activation mechanism of bimetallic MOF for water contaminant degradation: a review. *Molecules.* 2023;28(8):3622. doi: 10.3390/molecules28083622
20. Khan MS, Shahid M. Synthesis of metal-organic frameworks (MOFs): routes to various MOF topologies, morphologies, and composites. *Electrochemical Applications of Metal-Organic Frameworks.*2022:17-35. doi: 10.1016/b978-0-323-90784-2.00007-1
21. Hou X, Sun J, Lian M, et al. Emerging Synthetic Methods and Applications of MOF Based Gels in Supercapacitors, Water Treatment, Catalysis, Adsorption, and Energy Storage. *Macromolecular Materials and Engineering.* 2023;308(2):2200469.
22. He H, Li R, Yang Z, et al. Preparation of MOFs and MOFs derived materials and their catalytic application in air pollution: A review. *Catalysis Today.* 2021;375:10-29.
23. Al Amery N, Abid HR, Al-Saadi S, Wang S, Liu S. Facile directions for synthesis, modification and activation of MOFs. *Mater Today Chem.* 2020;17:100343.doi: 10.1016/j.mtchem.2020.100343
24. Johnson BA, Bhunia A, Fei H, Cohen SM, Ott S. Development of a UiO-type thin film electrocatalysis platform with redox-active linkers. *J Am Chem Soc.* 2018;140(8):2985-2994. doi: 10.1021/jacs.7b13077
25. Hu J, Liu Y, Liu J, Gu C, Wu D. High CO_2 adsorption capacities in UiO type MOFs comprising heterocyclic ligand. *Microporous Mesoporous Mater.* 2018;256:25-31. doi: 10.1016/j.micromeso.2017.07.051
26. Ma J, Chen Z, Diao Y, et al. Current and promising applications of UiO-based MOFs in breast cancer therapy. *Reactive and Functional Polymers*. 2024:105918.doi: 10.1016/j.reactfunctpolym.2024.105918
27. Vahabi AH, Norouzi F, et al. Functionalized Zr-UiO-67 metal-organic frameworks: Structural landscape and application. *Coordination Chemistry Reviews*. 2021; 445:214050. doi: 10.1016j.ccr.2021.214050
28. Hang C, Akpinar I, Qin Y, et al. A Review on Adsorption of Organic Pollutants from Water by UiO-67 and Its Derivatives. *J Nanoelectron Optoelectron.* 2021;16(12):1861-1873.
29. Ahmad K, Nazir MA, Qureshi AK, et al. Engineering of Zirconium based metal-organic frameworks (Zr-MOFs) as efficient adsorbents. *Mater Sci Eng B.* 2020;262:114766. doi: 10.1016/j.mseb.2020.114766
30. Flores-Cervantes DX, Medina-Montiel C, Ramirez-Corona N, Navarro-Amador R. Zirconium Based MOFs

and Their Potential Use in Water Remediation: Current Achievements and Possibilities. *Air, Soil and Water Research.* 2022;15(1):11786221221080183. doi: 10.1177/11786221221080183

31. Hobday CL, Marshall RJ, Murphie CF, et al. A Computational and Experimental Approach Linking Disorder, High Pressure Behavior, and Mechanical Properties in UiO Frameworks. *Angew Chem Int Ed Engl*. 2016 Feb 12;55(7):2401-2405. doi: 10.1002/anie.201509352
32. Liang W, Coghlan CJ, Ragon F, Rubio-Martinez M, D'Alessandro DM, Babarao R. Defect engineering of UiO-66 for CO_2 and H_2O uptake–a combined experimental and simulation study. *Dalton Transactions*. 2016;45(11):4496-4500. doi: 10.1039/c6dt00189k
33. Cavka JH, Jakobsen S, Olsbye U, et al. A new zirconium inorganic building brick forming metal organic frameworks with exceptional stability. *J Am Chem Soc.* 2008;130(42):13850-13851. doi: 10.1021/ja8057953
34. Chavan S, Vitillo JG, Gianolio D, et al. H_2 storage in isostructural UiO-67 and UiO-66 MOFs. *Phys Chem Chem Phys.* 2012;5:1614-1626.
35. Katz MJ, Brown ZJ, Colon YJ, et al. A facile synthesis of UiO-66, UiO-67 and their derivatives. *Chem Commun.* 2013;49(82):9449-9451. doi: 10.1039/c3cc46105j
36. Alavijeh RK, Beheshti S, Akhbari K, Morsali A. Investigation of reasons for metal–organic framework's antibacterial activities. *Polyhedron.* 2018;156:257-278. doi: 10.1016/j.poly.2018.09.028
37. Liu, Jianghua, Di Wu, Niu Zhu, Yongning Wu, Guoliang Li. Antibacterial mechanisms and applications of metal-organic frameworks and their derived nanomaterials. *Trends Food Sci Technol.* 2021;109:413-434. doi: 10.1016/j.tifs.2021.01.012
38. Xu X, Ding M, Liu K, et al. The synthesis and highly effective antibacterial properties of Cu-3, 5-dimethy l-1, 2, 4- triazole metal organic frameworks. *Front Chem*. 2023;11:1124303.
39. El-Shahawy AAG, Dief EM, El-Dek SI, et al. Nickel-gallate metal–organic framework as an efficient antimicrobial and anticancer agent: *in vitro* study. *Cancer Nano.* 2023;14(1):60.doi: 10.1186/s12645-023-00207-5
40. Nakhaei M, Akhbari K, Kalati M, Phuruangrat A. Antibacterial activity of three zinc-terephthalate MOFs and its relation to their structural features. *Inorganica Chimica Acta*. 2021;522:120353. doi: 10.1016/j.ica.2021.120353
41. Ma S, Zhang M, Nie J, et al. Design of Double-Component Metal-Organic Framework Air Filters with PM2.5 Capture, Gas Adsorption and Antibacterial Capacities. *Carbohydrate Polymers.* 2019;203:415-422. doi: 10.1016j.carbpol.2018.09.039
42. Tabassum N, Kumar D, Verma D, Bohara RA, Singh MP. Zirconium oxide (ZrO_2) nanoparticles from antibacterial activity to cytotoxicity: A next-generation of multifunctional nanoparticles. *Mater Today Commun.* 2021;26:102156. doi: 10.1016/j.mtcomm.2021.102156
43. Liu W, Pan Y, Zhong Y, et al. A multifunctional aminated UiO-67 metal-organic framework for enhancing antitumor cytotoxicity through bimodal drug delivery. *Chem Eng J.* 2021;412:127899. doi: 10.1016/j.cej.2020.127899
44. Chen DT, Bi JR, Wu J, Kumar A. Zirconium Based Nano Metal–Organic Framework UiO-67-NH2 with High Drug Loading for Controlled Release of Camptothecin. *J Inorg Organomet Polym.* 2020;30(2):573-579. doi: 10.1007/s10904-019-01188-y
45. Zheng Y, Zhang X, Su Z. Design of metal–organic framework composites in anti-cancer therapies,. *Nanoscale.* 2021;13:12102-12118. doi: 10.1039/d1nr02581c
46. Febrian MB, Mahendra I, Kurniawan A, et al. Zirconium doped hydroxyapatite nanoparticle as a potential design for lung cancer therapy. *Ceramics International.* 2021;47(19):27890-27897. doi: 10.1016/j.ceramint.2021.06.219
47. Han I, Choi SA, Lee DN. Therapeutic Application of Metal–Organic Frameworks Composed of Copper, Cobalt, and Zinc: Their Anticancer Activity and Mechanism. *Pharmaceutics*. 2022;14(2):378. doi: 10.3390/pharmaceutics14020378
48. Sun Y, Chen Y, Ma X, et al. Mitochondria-Targeted hydroxyapatite nanoparticles for selective growth inhibition of lung cancer *in vitro* and *in vivo. ACS Appl Mater Interfaces.* 2016;8(39):25680-25690. doi: 10.1021/acsami.6b06094
49. Xiong H, Du S, Ni J, Zhou J, Yao J. Mitochondria and nuclei dual-targeted heterogeneous hydroxyapatite nanoparticles for enhancing therapeutic efficacy of doxorubicin. *Biomaterials.* 2016;94:70-83. doi: 10.1016/j. biomaterials.2016.04.004
50. Di Virgilio AL, Arnal PM, Maisuls I. Biocompatibility of core@shell particles: cytotoxicity and genotoxicity in human osteosarcoma cells of colloidal silica spheres coated with crystalline or amorphous zirconia. *Mutat Res Genet Toxicol Environ Mutagen*. 2014;770:85-94. doi: 10.1016/j.mrgentox.2014.05.009
51. Karunakaran G, Suriyaprabha R, Manivasakan P, Yuvakkumar R, Rajendran V, Kannan N. Screening of in vitro cytotoxicity, antioxidant potential and bioactivity of nano- and micro-ZrO_2 and -TiO_2 particles. *Ecotoxicol Environ Saf.* 2013;93:191-197.
52. Aude-Garcia C, Dalzon B, Ravanat JL, et al. A combined proteomic and targeted analysis unravels new toxic mechanisms for zinc oxide nanoparticles in macrophages. *J Proteomics.* 2016;134:174-185. doi: 10.1016/j.jprot.2015.12.013